J Electroceram (2006) 16:307–311
DOI 10.1007/s10832-006-9870-8

Behavior of piezoelectric ultrasonic tubular transducers in relation to tube geometry

N. K. C. Ng · T. Li · J. Ma · F. Y. C. Boey

Abstract The piezoelectric ultrasonic actuator, a recent development in the field of ferroelectrics, has led to applications in a wide range of industries. These actuators have proven to outperform their electromagnetic counterparts of mm-order diameters and below, and the demand for such devices in high power applications continues to increase. The performance of such motors, in particular, those of tubular form, are governed by two key material properties, the mechanical quality factor, Q_m and the piezoelectric constant, d_{31}. This paper presents experimental results showing that the factor, $Q_m \times d_{31}$, indeed governs the performance of such motors. In the present work, tubes of various materials and geometries are characterized in terms of resonance frequency, the dynamic bending displacement, and the vibration velocity. A comparison is made showing a possible dependence of material constants, Q_m and d_{31} on the geometry of the tube, as well as the input electric field. The derivation of the constitutive relationships has been carried out and compared to the experimental results. The geometric dependence of material property data indicates the need for a possible relationship linking these properties to the geometry. The second part of the work presents experimental data verifying the relationship between the material properties Q_m and d_{31}, with the geometry of the material and the input electric field.

Keywords Piezoelectric · Ultrasonic · Transducer

1 Introduction

Piezoelectrics belong to a class of materials which exhibit deformation in response to an external electric field, a phenomenon first observed in 1880 by Jacques and Pierre Curie [1]. In recent years, ultrasonic actuators of tubular form have been developed, which outperform their electrostatic counterparts at sizes of mm-order dimensions and below [2]. The focus of this work is to develop relationships between actuator performance and the material properties, and secondly, to understand how the material properties scale with the geometry, thereby paving the way for development towards miniaturized applications.

Piezoelectric ultrasonic transducer performance is a function of two key material properties, the piezoelectric constant, d_{31}, which governs the strain per unit of voltage input to the material, and secondly, the mechanical quality factor, Q_m. The piezoelectric effect arises from electric dipoles in the material, and neighbouring dipoles tend to align with each other, forming regions of local alignment, or Weiss domains, resulting in a net polarization. Both lattice deformation of individual grains, and the changes in the ferroelectric domain populations contribute to the piezoelectric response [3]. The domain walls have a significant influence on the properties of PZT ceramics [4]—under the application of an electric field, domain walls move so as to minimize domain energy. The result is a change in the domain structure (size, shape and population), and therefore a change in the net strain and polarization [5].

A piezoelectric material may be doped with small quantities of a *donor dopant* to create metal (cation) vacancies in the crystal structure. This facilitates domain wall motion thereby improving its piezoelectric properties (such as the piezoelectric **d** constant) [6], but at the expense of the mechanical quality factor, Q_m, whose physical meaning can be defined as the reciprocal of the internal friction of the dipoles [7], or the damping in the material due mechanical loss such as internal friction. Piezoceramics described as such are categorized as *soft ceramics*, while *hard ceramics*, on the other

N. K. C. Ng (✉) · T. Li · J. Ma · F. Y. C. Boey
Nanyang Technological University, School of Materials Science & Engineering

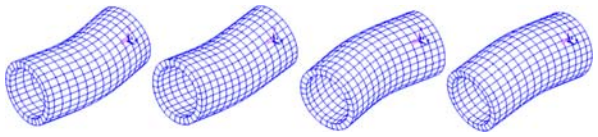

Fig. 1 Bending vibration of PZT Tube (L20 mm × OD10 mm × ID8 mm, $f_r = 51$ kHz)

hand are doped with a*cceptor dopants*, which create oxygen (anion) vacancies in the crystal structure. In hard PZT, domain walls are pinned by impurities, whereas soft PZT is characterized by mobile domain walls [8].

Kurosawa [2, 9] describes tubular-type actuators consisting of a tube of piezoelectric material coated internally and externally with a layer of electrode. The inner diameter of the tube is coated with a single inner-electrode, and the outer-electrode is quartered. Voltages applied to each of the four outer electrodes are sinusoidal, each with a 90 degree phase lag behind the other.

The bending motion of the piezoelectric tube causes a point at the end of the tube to move in a circular fashion (Fig. 1), and if a conical "end cap" contacts the tube at this point, the rotational motion can be converted to useful output. Under a "no slip" condition, the contact point of the "end cap" will move at the same velocity as the point at the edge of the PZT tube. Under this assumption, the rotational speed of the motor (in rpm), is directly related to the bending displacement and resonance frequency by the relationship [10]:

$$\omega_{\text{motor}} = \frac{60 f_r \zeta}{r_{\text{contact}}}, \tag{1}$$

where r_{contact} is the radius from the axis of rotation to the point of contact between the tube and the "end cap," f_r is the resonance frequency, and ζ is the bending displacement of the tube. This "contact point" moves in a circular fashion and the speed at which it moves is equal to the vibration velocity, $v_v = \omega_r \times \zeta$ or $2\pi f_r \zeta$, which is directly related to motor speed.

2 Theory

The performance of a piezoelectric ultrasonic motor is governed by the performance of the piezoelectric tube (i.e., the piezoelectric tubular transducer) and the vibration velocity of the point on at the end of the tube sets the upper limit to the speed of the motor. The vibration velocity, $v_v = 2\pi f_r \zeta$, requires f_r and ζ to be obtained, which may be derived from the Timoshenko Beam Theory [2, 11–15]. In Timoshenko beam theory, an element of the beam is modeled having a transverse motion with a shear deformation and a rotation. Under the action of a shear force, F, and a bending moment, M, a transverse displacement, ζ, and a rotation, φ, are produced, and the element of density ρ deforms by an angle γ. The equation of motion given by the Timoshenko model is [15]:

$$Y^E I \frac{\partial^4 \zeta}{\partial x^4} + \rho A \frac{\partial^2 \zeta}{\partial t^2} - \rho I \left(1 + \frac{Y^E}{kG}\right) \frac{\partial^4 \zeta}{\partial x^2 \partial t^2} + \frac{\rho^2 I}{kG} \frac{\partial^4 \zeta}{\partial t^4} = 0 \tag{2}$$

where the moment of inertia, $I = \frac{\pi}{64}(D^4 - d^4)$, A is the cross sectional area, D and d are the outer and inner diameters, k is the shape factor, and G is the shear modulus.

The solution to the Timoshenko beam model [12] is of the form:

$$\begin{bmatrix} \zeta(x) \\ \varphi(x) \end{bmatrix} = \begin{bmatrix} C_1 \\ D_1 \end{bmatrix} \sin ax + \begin{bmatrix} C_2 \\ D_2 \end{bmatrix} \cos ax + \begin{bmatrix} C_3 \\ D_3 \end{bmatrix} \sinh bx + \begin{bmatrix} C_4 \\ D_4 \end{bmatrix} \cosh bx \tag{3}$$

where C_i, $D_i (i = 1 \text{ to } 4)$, a and b are constants that can be determined.

The boundary conditions for the free-free end conditions are applied:

$$\begin{cases} \dfrac{d\zeta}{dx} - \varphi = 0 & \text{at } x = 0, \text{ and } x = 1 \\ \dfrac{d\varphi}{dx} = 0 & \text{at } x = 0, \text{ and } x = 1 \end{cases} \tag{4}$$

By doing so, it can be shown that the bending-mode resonance frequency [15] is given by:

$$f_r = \frac{\sqrt{Y^E}\sqrt{a^2 - b^2}}{2\pi L \sqrt{\rho\,(5 + 3\sigma)}}, \tag{5}$$

where Y^E is the Young's Modulus, ρ is the density, and σ is the Poisson's ratio, and the wave numbers a and b are to be obtained by solving the simultaneous equations by numerical methods:

$$\begin{cases} \dfrac{(a^2 - b^2)(a^2 + b^2 + \gamma^2 ab - ab)(a^2 + b^2 - \gamma^2 ab + ab)}{2ab(b^2 + \gamma^2 a^2)(a^2 + \gamma^2 b^2)} \\ \qquad \times \sin a \sinh b - \cos a \cosh b + 1 = 0 \\ \dfrac{(\gamma^2 b^2 + a^2)(\gamma^2 a^2 + b^2)}{(a^2 - b^2)(1 + \gamma^2)} = s^2 = \dfrac{16L^2}{D^2 + d^2} \end{cases} \tag{6}$$

where $\gamma = \sqrt{4 + 3\sigma}$, s is the shape factor, L is the tube length, D and d are the outer and inner diameters respectively.

Similarly, the formula for the bending displacement at resonance [15] may be evaluated as:

$$\zeta = Q\frac{16d_{31}V \times l \times (L-l)\cos\beta}{\pi(D^2+d^2)\ln\frac{D}{d}} \tag{7}$$

where d_{31} is the piezoelectric constant, V is the voltage applied to the electrode, β is 45° (for a 4-electrode tube), l is the distance from the nodal point to the end of the tube.

Here, the mechanical quality factor, Q, is defined as the 2π multiplied by the ratio of energy stored to the energy dissipated per cycle. This is analogous to the spring-mass damper system, where the ratio is given by:

$$\begin{aligned} Q &= 2\pi\frac{\textit{energy stored in the spring}}{\textit{energy dissipated per cycle}} \\ &= 2\pi\frac{\frac{1}{2}m\omega^2X^2}{\left[\frac{1}{2}c\omega^2X^2\right]\frac{2\pi}{\omega}} = \frac{1}{2\zeta} \end{aligned} \tag{8}$$

where ζ is the damping ratio, m is the mass, c is the constant of proportionality for the dashpot, X is the amplitude, and ω is the frequency. Q is numerically equivalent to the ratio of the displacement at resonance to the static displacement, and may also be approximated by

$$Q_m = f_r/\Delta f, \tag{9}$$

where f_r is the resonance frequency, and Δf is the band width at 3 dB corresponding to an amplitude reduction of $1/\sqrt{2}$ in relation to the amplitude at resonance. The piezoelectric equivalent circuit (consisting of a capacitor in parallel with a resistor, inductor, and another capacitor [16]) presents another analogy, with the mechanical quality factor, Q_m given by:

$$Q_m = \frac{\text{energy stored in a period (in } L \text{ and } C)}{\text{energy dissipated in a period (in } R)} \tag{10}$$

In this case, the sharpness of the resonance peak, $Q_m = f_r/\Delta f$, applies to the admittance maximum and not the displacement maximum.

By substituting f_r and ζ, into the vibration velocity equation, $v_v = 2\pi f_r\zeta$, it can be shown that

$$\begin{aligned} v_v = {} & \frac{16}{\pi}(V\cos\beta) \\ & \times\left(Qd_{31}\sqrt{\frac{Y^E}{\rho(5+3\sigma)}}\right)\left(\frac{L\times\frac{l}{L}\left(1-\frac{l}{L}\right)\sqrt{a^2-b^2}}{\left(D^2+d^2\right)\ln\frac{D}{d}}\right) \end{aligned} \tag{11}$$

In this manner, the vibration velocity has been expressed in terms of 3 parameters: $V\cos\beta$, an electrical-related factor, a materials-related factor,

$$Qd_{31}\sqrt{\frac{Y^E}{\rho(5+3\sigma)}}, \quad \text{and} \quad \frac{L\times\frac{l}{L}\left(1-\frac{l}{L}\right)\sqrt{a^2-b^2}}{\left(D^2+d^2\right)\ln\frac{D}{d}},$$

a geometry-related factor. It should be noted that there is some cross-coupling between the nodal point term, $\frac{l}{L}(1-\frac{l}{L})$, and the wave number term, $\sqrt{a^2-b^2}$, which depend slightly on the Poisson ratio, σ. However, based on data from commercial piezoelectric materials (APC International Ltd, Boston Piezo Optics, Channel Industries, Morgan Electroceramics, Piezo Kinetics, & Saint-Gobain Quartz), it was found that assuming a Poisson Ratio of $\sigma = 0.30$, would not affect the parameter, $\frac{l}{L}(1-\frac{l}{L})$, by more than 1% and $\sqrt{(a^2-b^2)}$ by 3%. The parameter, $Qd_{31}\sqrt{\frac{Y^E}{\rho(5+3\sigma)}}$, is of particular interest because it isolates the material performance from the geometry. By differentiating the vibration velocity with respect to the voltage, we have:

$$\begin{aligned} \frac{dv_v}{dV} = {} & \frac{16\cos\beta}{\pi} \times \textit{Material Factor} \\ & \times \textit{Geometric Factor} \end{aligned} \tag{12}$$

and $\mathrm{d}v_v/\mathrm{d}V$ may then be plotted against the geometric factor to obtain the experimental "material factor."

3 Experimental procedure

PZT tubes of *hard* PZT-III and *soft* PZT-VI were obtained from Boston Piezo Optics, who machined tubes from select, void-free high quality raw PZT billets. The process used was ultrasonic machining, whereby erosion of the material occurs by means of fine abrasive grains in a slurry injected between the workpiece and the tool [17]. The process is gentle on the tube walls, minimizes surface imperfections, and does not produce a heat-affected zone, nor does it cause any surface chemical/electrical alterations. The tubes were obtained from the vendor, poled with quartered electrodes on the outer surface, and a single inner electrode.

The initial resonance frequency is calculated by formula and verified by a HP4194A impedance analyzer. The PZT tube is mounted horizontally at its nodal points using rubber O-rings and sinusoidal voltages are applied by means of a Yokogawa FG300 function generator which outputs two sinusoidal waveforms, 90 degrees phase difference apart. The output is coupled to 2 high voltage amplifiers (Trek PZD2000) and these are connected to pairs of opposite-facing electrodes on the piezoelectric tube. Non-contact bending displacement measurement of the tube is measured by the

MTI2000 Fotonic Sensor, and the displacement & frequency output captured on an oscilloscope. A metallic foil placed on the piezoelectric tube allows the displacement to be picked up by the probe.

The vibration velocity was determined from $v_v = 2\pi f_r \zeta$, and plotted against voltage for each tube. From the linear portion of this curve (up to electric fields of about 100 V/mm on average), the gradient $\mathrm{d}v_v/\mathrm{d}V$ is obtained, and plotted against the geometric factor. By doing so, we wish to verify that the $\mathrm{d}v_v/\mathrm{d}V$ vs. geometric factor plot is a straight line, with the gradient being a constant that is proportional to the material factor, and the constant of proportionality being numerical equal to $(16\cos\beta)/\pi$.

4 Results and discussion

A comparison of the normalized resonance frequency parameter, $2\pi L f_r(\rho/Y^E)^{1/2}$ as a function of the inverse of the shape factor, $1/s = \sqrt{\frac{D^2+d^2}{16L^2}}$, is shown (Fig. 2).

The numbers listed refer to the dimensions of the tubes (Length-OD-ID) in mm. A slight shift in the resonance frequency is experienced as the voltage is increased, but this shift is small enough that there is reasonable agreement between the experimental and theoretical values.

Vibration velocity vs. geometrical factor

The results for $\mathrm{d}v_v/\mathrm{d}V$ plotted against the geometric factor for *hard* PZT (PZT-III) and *soft* PZT (PZT-VI) yielded linear relationships (Fig. 3):

Each point is labeled with its dimensions in *length-OD-ID*, together with the resonance frequency (as some material properties may be frequency-dependent). Higher vibration velocities are observed in *hard* PZT, due to lower internal friction made possible by the pinning of domain walls (and hence lower domain wall mobility). Tubes of *hard* PZT Navy

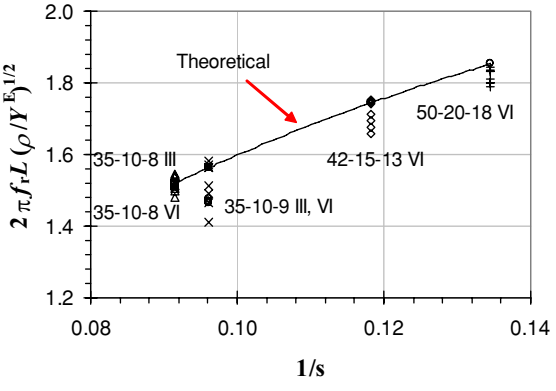

Fig. 2 Theoretical & resonance frequencies of tubes of PZT-III & PZT-VI

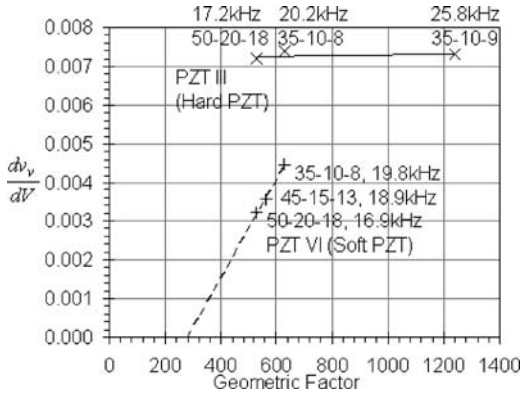

Fig. 3 $\mathrm{d}v_v/\mathrm{d}V$ vs. Geometric factor

Type III did not behave as expected, instead, $\mathrm{d}v_v/\mathrm{d}V$ appears to be independent of the geometric factor. *Soft* PZT Navy Type VI/High Density materials followed the relationship more closely, with the linear y-intercept passing not too far from the origin.

It is believed that the difference between the behavior of *hard* and *soft* PZT comes from cross-coupling in either Q or d_{31} with the other parameters. Other material properties, Y_E, ρ, σ are unlikely candidates due to the matching of the theoretical and experimental values of the resonance frequency, f_r. Since $\mathrm{d}v_v/\mathrm{d}V$ was obtained from the linear portion of the curve, dependence of these coefficients on the electric field as indicated by the Rayleigh Law (now also observed in soft ferroelectric materials, [18–19]) is not expected to be a factor. Both Q and d_{31} are functions of the domain wall motion, which has shown to exhibit a frequency dependence [20]. At large geometric factors, the resonance frequencies are higher, switching time for domains to change could be reduced [20], hence a reduced piezoelectric response.

5 Conclusion

The relationships derived for piezoelectric ultrasonic tubular transducers indicate $Q_m \times d_{31}$ as a primary material property that relates to its performance (and in existing commercially available materials, this value is largest in *hard* PZT). Experimental verification of the resonance frequency is provided. A relationship for the vibration velocity of piezoelectric tubular transducers has been proposed. *Soft* PZT followed the linear trend predicted by this relationship, but the reasons for the deviation in *hard* PZT are less clear, notwithstanding the apparent independence of $\mathrm{d}v_v/\mathrm{d}V$ from the geometric factor. Further analysis is proposed to obtain more data, to determine the limits of the linear relationship, to develop an explanation this phenomenon, and to determine if the effect of frequency (due to a change in geometry) fully explains the reasons for this phenomenon. If this is indeed caused by

the frequency dependence of the domain wall mobility [20], an understanding of how the material properties Q and d_{31} scales with the resonance frequency or the geometry of a sample is important in the development of piezoelectric material, particularly when a change in the form factor or size is required. This result has wide-reaching implications because if the apparent geometric independence in PZT-III extends to miniaturized dimensions it will mean that applications at a small scale would have the same high vibration velocities as those on a much larger scale.

References

1. W.G. Cady, *Piezoelectricity* (Dover Pub., New York, 1964).
2. T. Morita, M.K. Kurosawa, and T. Higuchi, *Sens and Actuators A: Phys.*, **83**(1–3), 225–230 (2000).
3. S. Li, W. Cao, and L.E. Cross, *J. Appl. Phys*., **69**, 7219 (1991).
4. Q.M. Zhang, H. Wang, N. Kim, and L.E. Cross, *J. Appl. Phys*., **75**, 454 (1994).
5. S. Sherrit, H.D. Wiederick, B.K. Mukherjee, and M. Sayer, *Proc. SPIE*, **99**, 3040 (1997).
6. B.H. Chen, C.L. Huang, and L. Wu, *Solid State Electronics*, **48**, 2293–2297 (2004).
7. C.L. Huang, B.H. Chen, and L. Wu, *Solid State Communications*, **130** 19–23 (2004).
8. Q.M. Zhang, W.Y. Pan, and L.E. Cross, *J. Appl. Phys*., **63**, 2492 (1988).
9. M. Kurosawa, K. Nakamura, T. Okamoto, and S. Ueha, *IEEE Trans. On UFFC*, **36**(5), 517–521 (1989).
10. Y. Chen, and J. Guo, (Zhejiang University Press. Chinese, 1994).
11. H.-P. Lin, and S.C. Chang, *J. Sound and Vib*., **281** 155–169 (2005).
12. S.M. Han, H. Benaroya, and T. Wei, *J. Sound and Vib*., **225**, 935–988 (1999).
13. S.P. Timoshenko, *Philos. Mag. Series 6*, **41**, 744–746 (1921).
14. S.P. Timoshenko, *Philos. Mag. Series 6*, **43**, 125–131 (1922).
15. T. Li, Ph.D. Thesis, Nanyang Technological University (2003).
16. IEC Standard 302 Standard definitions and methods of measurement for piezoelectric vibrators operating over the frequency range up to 30MHz. (1969)
17. S. Kalpakjian, *Manuf. Eng. and Tech*., 3rd Ed. (Addison-Wesley, 1995).
18. S. Bhaskar, S.B. Majumder, P.S. Dobal, and R.S. Katiyar, *J. Appl. Phys*., **89**(10), 5637–5643 (2001).
19. D. Damjanovic, and M. Demartin, *J. Phys. D: Appl. Phys*, **29**(7), 2057–2060 (1996).
20. A.J. Masys, W. Ren, G. Yang, and B.K. Mukherjee, *J. Appl. Phys*., **94**(2), 1155–1162 (2003).